JOURNAL OF MATERIALS SCIENCE **33** (1998) 5029–5036

On the effects of surface treatments on the mechanical strength of carbon fibres

P. BERTRAND, M-H. VIDAL-SÉTIF, R. VALLE, R. MÉVREL
Direction des Matériaux, Office National d'Etudes et de Recherches Aérospatiales (ONERA) 29 avenue de la Division Leclerc, F-92322 Châtillon, France

TiB_2, pyrolytic carbon (C_{pyr}) and $C_{pyr} + TiB_2$ double layer coatings have been envisaged as potential protective coatings to prevent the deleterious interface reactions between the carbon fibre and the aluminium matrix during composite manufacturing. These coatings have been obtained by low pressure chemical vapour deposition on T800H carbon fibre yarns. In spite of a 20% increase in the coated monofilaments tensile strength observed for very thin C_{pyr} coatings, a strength decrease as a function of the coating thickness is recorded for single C_{pyr} or TiB_2 layers. For the TiB_2 coatings, this decrease fits well with Ochiai's model which simulates the notch effect induced by a cracked brittle layer. Concerning the C_{pyr} coatings, a lower damaging effect is observed as compared to TiB_2, it may be explained by the difference between the Young's moduli of both layers. Although the initial fibre properties are not perfectly maintained in the case of the double layer, the crack deviation role of the C_{pyr} coating succeeds in preserving the coated fibres from the TiB_2 notch effect, thus leading to a noticeable strength increase.

1. Introduction

Carbon fibre reinforced aluminium composites are expected to make progress in the application as light structural materials owing mainly to the advantage of a good dimensional stability at high temperatures in addition to their mechanical properties such as high specific strength and modulus.

However, manufacturing problems have slowed down their industrial development. For instance, interface chemical reactions between fibre and matrix often take place during composite manufacturing. This is especially serious when using poly-acrylonitrile (PAN)-based high strength type carbon fibres produced at a relatively low temperature [1, 2]. The reaction which leads to the formation of aluminium carbides Al_4C_3, is known as one of the causes reducing the composite strength because these brittle crystals can act as stress concentration sites possibly leading to crack initiation and propagation [3].

One approach to overcome these deleterious fibre matrix interface reactions is to develop an inert barrier coating on the fibre [4]. The titanium diboride coating (TiB_2), which is used as a cathode material in the electrolytical production of aluminium owing to its high chemical inertness at high temperature [5, 6], could be a good candidate for aluminium metal matrix composites (MMC) applications. It could both promote wettability between the carbon fibre and the aluminium matrix and confer an adequate protection against the formation of the aluminium carbides (chemical barrier).

Nevertheless, different studies have shown that when a fibre is coated with a brittle material, the coated fibre strength is generally reduced [7, 8]. This effect is attributed to the propagation of the cracks initiated by premature failure of the coating layer. Consequently, in order to avoid this degradation of the fibre properties which would be detrimental to the mechanical behaviour of the composite, we envisaged to deposit a double layer consisting of a pyrolytic carbon (C_{pyr}) inner layer and a TiB_2 outer layer. It is expected that the C_{pyr} coating, according to its microstructure based on units having their graphite basal planes parallel to the interface, would not lead to a decrease in the coated fibre strength because of its crack deviation function. Moreover, the use of the double layer should thus permit to fulfil both the physicochemical role (chemical barrier and wetting agent) and the mechanical role (mechanical fuse) required by the interphase in a composite application.

In the present work, we have focused our attention on the effect of the TiB_2 and double layer $C_{pyr} + TiB_2$ coatings on the strength of the coated Toray T800H fibre (high strength type carbon fibre, diameter $= 5\ \mu$m, axial Young's modulus 300 GPa, 6000 filaments yarn). In the case of the TiB_2 coatings, the main objective is to determine if a single TiB_2 layer could be used as a protective film without introducing any degradation of the fibre mechanical properties. Concerning the double layer investigation, it was firstly aimed at verifying whether the C_{pyr} coating, through its crack deviation function, could reduce the damaging effect provoked by TiB_2. Furthermore, different thickness combinations are taken into consideration in order to determine the influence of each layer on the coated fibre strength.

2. Experimental

2.1. Coating procedure

C_{pyr} and TiB_2 coatings have been deposited on unidirectional carbon fibre yarns using low pressure chemical vapour deposition (LPCVD), this process being one of the most convenient infiltration mode permitting to attain a homogeneous coating on each filament of a yarn. Then, the coated monofilaments have been submitted to tensile tests in order to follow the fibre strength evolution.

Details of the experimental apparatus used and the complete kinetics and morphological studies performed to optimize the infiltration process, are described elsewhere [9, 10]. A brief summary of the coating procedure will however be reported here.

Firstly, the fibre yarns are continuously heat-treated through a hot wall reactor to thermally remove the polymer sizing. This procedure is performed at 1073 K under reduced pressure (100 Pa). The coatings are subsequently carried out in two low pressure hot wall reactors [9, 10]. The reactor used for TiB_2 coatings is represented in Fig. 1.

Concerning the pyrolytic carbon deposition, ethylene is used as a hydrocarbon precursor with argon as a carrier gas. Temperature and pressure were varied about the values of 1398 K and 3 kPa to optimize the infiltration process, the growth rate and the morphology of the coatings. A typical laminar microstructure, exhibiting the characteristic Maltese cross under polarized light optical microscopy, is obtained thereby indicating that C_{pyr} forms with its basal planes parallel to the fibre surface [11]. Furthermore, the turbostratic structure of the C_{pyr} coating has been evidenced through transmission electron microscope (TEM) observations [12].

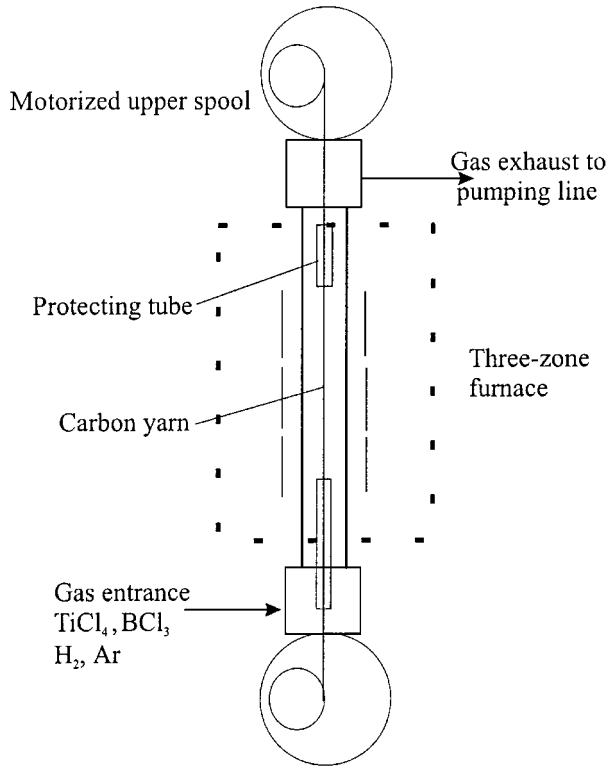

Figure 1 Schematic diagram of the low pressure chemical vapour deposition reactor used for TiB_2 coatings.

Regarding the TiB_2 coating, the reactants and reaction used, are as follows:

$$TiCl_4\,(g) + 2\,BCl_3\,(g) + 5\,H_2\,(g) \rightarrow TiB_2\,(s) + 10\,HCl\,(g)$$

The operating conditions ($T = 1073$ K, $P = 400$ Pa, Ti/B = 0.5, H/Cl = 10) were selected in order to deposit pure TiB_2 without a boron co-deposit and with a growth rate consistent with a continuous infiltration treatment of the yarn [10].

One of the main difficulties encountered during this investigation was to estimate, in order to analyse the thickness effect on the fibre strength, coating thicknesses as thin as a few tens of nanometers and their homogeneity throughout the yarn. Ideally, it requires to determine, on a significant number of filaments, the coating thickness both in the core and in the peripheric zones of the yarns. This investigation was performed in a high resolution scanning electron microscope (SEM) on nickel infiltrated polished cross-sections of the yarns [10]; however, this procedure has proved to be too lengthy for obtaining statistically significant results. So, the quality and measurement of the infiltration was checked on thicker coatings, easier to observe, obtained by lower spooling speeds. The required thickness is then derived by an adjustment of this speed, assuming that the growth rate is a linear function of time in the reactive zone which seems to be confirmed by the mass evolution of the coated yarn as a function of this parameter [13]. For every measurement carried out with conditions corresponding to the low thicknesses under investigation, the observed values were in good agreement with the expected values (±10%), nevertheless their precision and homogeneity must be considered with care.

2.2. Tensile strength characterization

In order to evaluate the mechanical properties of the carbon fibre as a function of the treatments, we measured the strength evolution of the coated monofilaments. For that, tensile tests were performed with a microtensile testing machine designed at ONERA [14]. The fibre, taken at random within the coated yarn, is stuck on a polyester holder, previously cut in accordance with the effective test length envisaged. A centering device allows to realize the satisfactory alignment which is essential for a good precision of the results. Fifty tests are carried out for each experiment with an effective gauge length of 10 mm and a crosshead rate of 0.07 mm/min.

Due to the brittle behaviour of the fibre fracture, the failure strength statistics may be represented by a three-parameter Weibull distribution based on the "weakest link hypothesis" where the strength is controlled by failure at the most serious defect. The probability of failure at stress σ is given by [15–17]

$$P_i(\sigma) = 1 - \exp\left[-L\left(\frac{\sigma - \sigma_u}{\beta}\right)^m\right] \qquad (2)$$

where m is the Weibull modulus representing the strength dispersion, σ_u the threshold stress below which the failure probability is zero, β the scaling parameter and L the fixed gauge length, assuming a constant diameter cylindrical geometry.

If the threshold stress σ_u is assumed to be equal to 0 [18], then

$$P_i(\sigma) = 1 - \exp\left[-\left(\frac{\sigma}{\sigma_0}\right)^m\right] \quad \text{where } \sigma_0 = \beta L^{-1/m} \tag{3}$$

A linear regression method is used to determine the Weibull parameters m and σ_0. The mean value $\bar{\sigma}$ is

$$\bar{\sigma} = \sigma_0 \Gamma(1 + 1/m) \tag{4}$$

where Γ is the gamma function.

Due to the high number of tests (N) taken into consideration in each case, the choice of the estimator is less critical; in the present case, the estimator used is $P_i(\sigma) = i/N + 1$.

3. Results and discussion

The results concerning each step of the treatment, i.e., unsizing, C_{pyr} deposition, TiB_2 deposition and $C_{pyr} + TiB_2$ double layer deposition, are summarized in Table I. Different thicknesses are considered in each case, they all seem to present a unimodal distribution of the defects except for the double layer with a 125 nm thick C_{pyr} coating. In order to determine the coatings influence on the fibre properties, the mean tensile strength is calculated for a given mean cross section of the uncoated fibre (diameter = 5 μm).

One first remark may be deduced from this table. Tensile tests performed on as-received and unsized T800H fibres reveal practically no effect of the thermal treatment. Despite the large number of filaments tested (100 in each case), the slight differences in Weibull moduli and mean tensile strengths do not seem to be significant.

TABLE I Weibull modulus and mean strength of monofilaments after different treatments

Fibre T800	Weibull modulus	Mean tensile strength (MPa)
Sized fibre	6.6	5250
Unsized fibre	5.5	5400
Unsized fibre + TiB_2 (75 nm)	4.4	1625
Unsized fibre + TiB_2 (56 nm)	6.3	1975
Unsized fibre + TiB_2 (45 nm)	5.3	2150
Unsized fibre + TiB_2 (28 nm)	5.6	3450
Unsized fibre + Cpyr (50 nm)	4.4	6000
Unsized fibre + Cpyr (100 nm)	10	4775
Unsized fibre + Cpyr (200 nm)	10.3	3750
Unsized fibre + Cpyr (50 nm) + TiB_2 (56 nm)	6.9	4250
Unsized fibre + Cpyr (125 nm) + TiB_2 (75 nm)	4	4725[a]
Unsized fibre + Cpyr (125 nm) + TiB_2 (150 nm)	5.6	4600[a]

[a]Values calculated considering a unimodal distribution to compare with the other results.

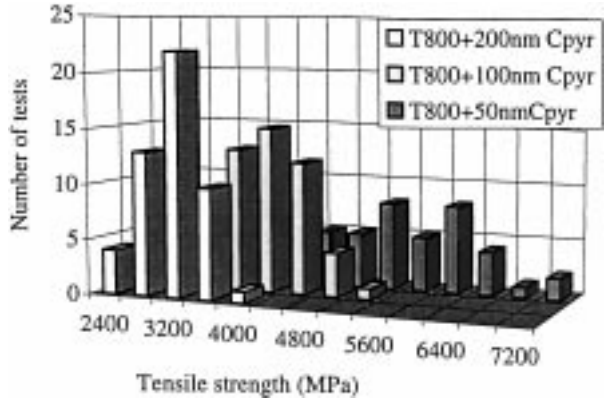

Figure 2 Tensile strength of the coated monofilaments as a function of the C_{pyr} coating thickness.

3.1. C_{pyr} coated fibres and TiB_2 coated fibres

Concerning the C_{pyr} coating, we first observe an increase in the tensile strength for a thickness of 50 nm as compared to the uncoated fibre (Fig. 2). This behaviour which has already been reported by Honjo *et al.* [19] on T300 fibres with 30 nm and 80 nm thick carbon coatings seems to result from the fibre surface defects removal by the carbon coating. In fact, carbon could be likely to fill in the pores located at the fibre surface, thus inhibiting the effects of stress concentrations due to this kind of rugosity (Fig. 3). However, when the C_{pyr} coating thickness increases, the coated fibre strength decreases to 3750 MPa for a 200 nm thick coating. This trend may be related to the evolution reported by Helmer *et al.* [20], from tensile tests performed on the whole T800H bundle, who notice an improvement of the coated fibre properties for a thickness of 16 nm and a degradation as soon as a thickness of 40 nm is attained. The origin of these discrepancies concerning the effect of the coating thickness cannot be clearly explained. They could have their origin either in the procedure of the mechanical tests (individual fibre or bundle tests and coating thickness measurement) or in the specific microstructure of the coatings.

We also remark a noticeable increase in the Weibull modulus with thicker C_{pyr} coatings (Table I). This result corresponds to a fibre strength dispersion sharpening about a mean value, which could derive from a change in the kind of defect leading to failure. Consequently, this failure could possibly be no more controlled by fibre surface defects but only by the presence of the C_{pyr} coating. However, in the case of a 50 nm thick film, both effects are supposed to coexist, given the observed fibre strength dispersion. This could mean that such a thin C_{pyr} coating (possibly further reduced by the 10% thickness dispersion inside the yarn) is unable to eliminate all fibre surface defects.

In the case of the TiB_2-coated fibres, an even more noticeable tensile strength decrease is observed as a function of the TiB_2-deposited thickness (Table I and Fig. 4). In fact, approximately the same fibre strengths

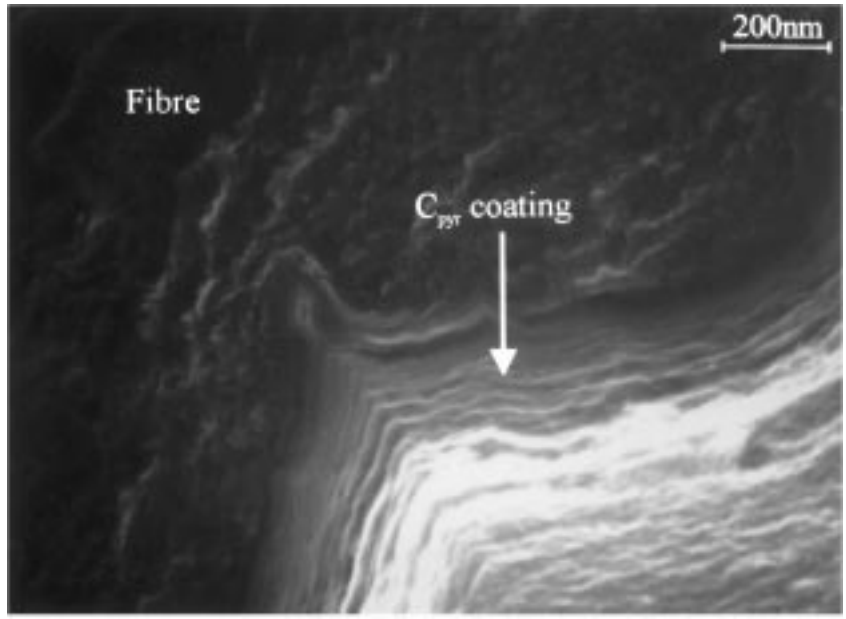

Figure 3 C_{pyr} coating filling the pores on the fibre surface and showing a stratified failure surface (section approximately perpendicular to the fibre axis).

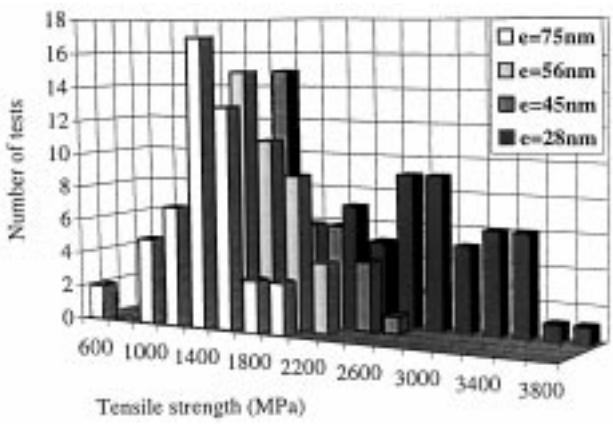

Figure 4 Tensile strength of the coated monofilaments as a function of the TiB_2 coating thickness (e).

are obtained with 28 nm thick TiB_2 and 200 nm thick C_{pyr} coatings. The relatively wide results dispersion, most probably due to thickness inhomogeneities, does not seem to depend, contrary to C_{pyr} films, on the coating thickness.

In order to analyse these evolutions, the experimental results have been compared to the Ochiai's model which established an analytical relation describing the strength damage of a composite consisting of a fibre coated with a cracked brittle layer, as a function of the coating thickness (Fig. 5a) [8]. In this model, the brittle layer is supposed to have the same mechanical properties (Young's modulus) as the fibre. According to the linear elastic fracture mechanics, the strength of the fibre (σ) and the fracture toughness (K_c) are related by the critical defect size (c) and a geometry-dependent factor $F(a/b)$ assuming the coated fibre as an isotropic

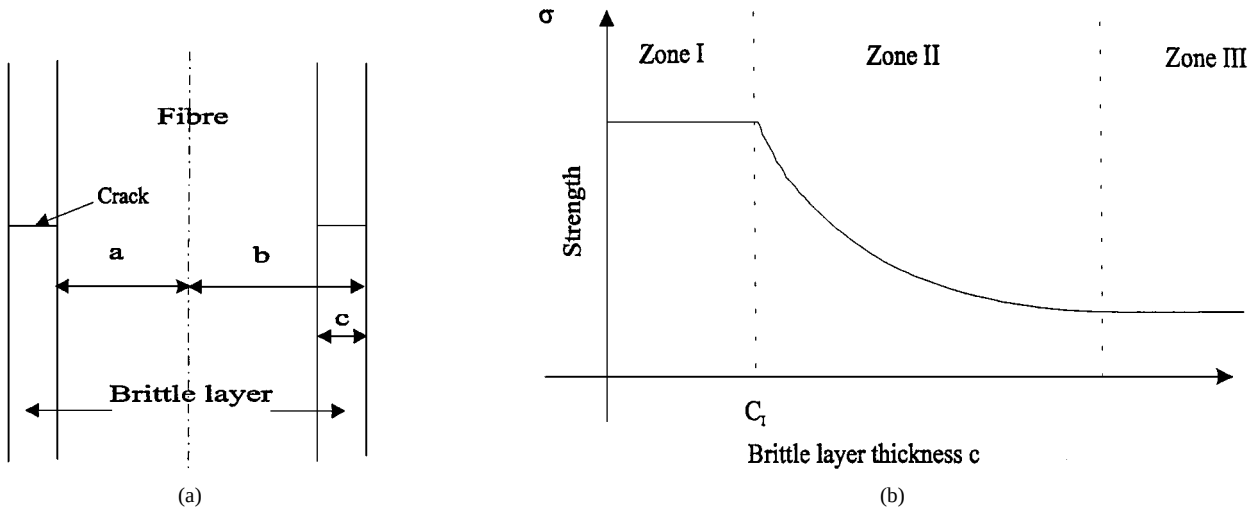

Figure 5 Ochiai's model of the coated fibre strength: (a) the circumferential crack in the brittle layer, (b) the fibre strength as a function of the brittle layer thickness [8].

and homogeneous cylindrical bar with an external circular notch (crack) [21].

$$K_c = \sigma\sqrt{\pi c}F\left(\frac{a}{b}\right) \tag{5}$$

Ochiai *et al.* distinguished three zones in the coated fibre strength plot as a function of the coating thickness (Fig. 5b):

- a first plateau which coincides with small thicknesses and where the presence of the brittle layer does not affect the fibre characteristics. In that case, the coated fibre failure most frequently results from the intrinsic defects of the fibre itself.
- when the thickness increases, the coated fibre strength decreases. The failure is attributed to the propagation in the fibre of the crack initiated in the brittle coating. In this zone, the coated fibre strength is a decreasing function of the brittle layer thickness c.

$$\sigma = \frac{V_f}{F\left(\frac{a}{b}\right)}\sqrt{\frac{E_f G_c}{\pi c}} \tag{6}$$

The transition between the two previous zones corresponds to a critical thickness defined by

$$c_I = \frac{G_c}{\pi\varepsilon_f^2 E_f\left[F\left(\frac{a}{b}\right)\right]^2} \tag{7}$$

where E_f, V_f, ε_f and $G_c = K_c^2/E_f$, respectively, represent the fibre modulus, the fibre volume fraction, the fracture strain of the uncoated fibre and the critical strain energy release rate of the fibre.

- finally, in the third zone, the layer is sufficiently thick so that the crack initiated by its failure immediately leads to the failure of the fibre.

We observe that, in the case of the TiB_2 coatings, the experimental results reported in Fig. 6 show a dependence of the fibre strength with the coatings thickness which fits well with zone 2 of this model. The fit of these

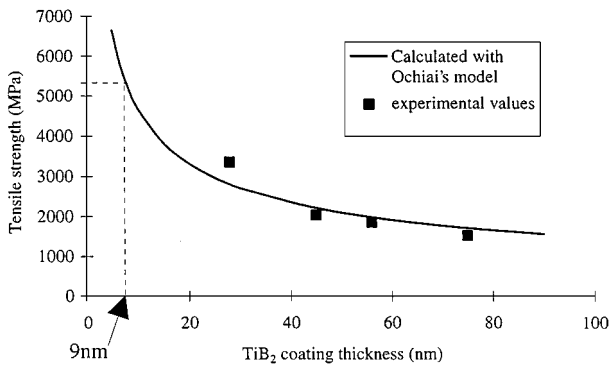

Figure 6 Tensile strength of the TiB_2 coated fibre as a function of the layer thickness compared to the Ochiai's model.

experimental data with the analytical relation (6) leads to a calculated value of the critical strain energy release rate of the fibre G_c of about 3 Jm^{-2} which is comparable to the values 2–3 J/m^{-2} and 1.8 J/m^{-2} reported, respectively, by Ochiai *et al.* [22] and Helmer *et al.* [20]. This observation confirms that the fibre failure mechanism could be due to a notch effect and associated with the propagation of a crack initiated in the coating. Although a circumferential crack was never observed experimentally by scanning electron microscopy (SEM) on the as-deposited films, it is likely that, as a result of the tensile stresses exerted on the TiB_2 layer due to the mismatch between thermal expansion coefficients (CTE), a crack could appear under a weak load during the tensile test. A calculation of the internal thermal residual stresses in the ceramic sheath, using a long perfectly bonded coaxial composite cylinder as a model (classical Lamé's solution), leads to high values. According to thermomechanical data and calculations which are discussed elsewhere [13], values of the axial tensile stresses in the TiB_2 coating in the range 2000 to 3000 MPa for thicknesses between 300 and 50 nm have been obtained. These values are of the same order of magnitude as the mechanical strength reported in the literature for thick TiB_2 coatings deposited by CVD [23], thereby justifying the possibility of a crack initiation when a tensile load is applied. The assumption put forward to explain the absence of cracks in the present as-deposited films is that the small size of the defects contained in very thin coatings leads to higher strengths than those reported in the literature.

The comparison with this model gives an estimate of the coating thickness above which a degradation of the fibre mechanical properties is likely to be recorded, i.e. about 10 nm for TiB_2 coatings (Fig. 6). Unfortunately, such a TiB_2 thickness cannot be envisaged as a single protection of the fibre because of the practical difficulties encountered for depositing uniform very thin coatings within a yarn given the fibre roughness and the unavoidable thickness dispersion during the infiltration process.

Concerning the C_{pyr} coating, we notice that fitting the experimental tensile strength data with the analytical relation (6) leads to a much too high value of the critical strain energy release rate of the fibre (G_c). However, comparing the internal thermal axial stress estimate of about 25 MPa in the C_{pyr} coating, with the tensile strength of C_{pyr} in the direction parallel to the interface (30 MPa [24]), a crack could possibly initiate during the early stage of the tensile test and a notch effect similar to that observed in the TiB_2 case would then be expected. In fact, the observed discrepancy between the experimental data and the Ochiai's model may have several origins.

First of all, the fact that the Ochiai's model is restricted to cases where the elastic properties of the coating layer are similar to those of the fibre ($E_{fibre} = 300$ GPa), may be considered as a severe limitation in the case of a C_{pyr} coating ($E_{Cpyr} = 30$ GPa). However, with a calculation method based on the concept of strain energy release rate using the shear lag analysis technique, Ochiai *et al.* [22] described the

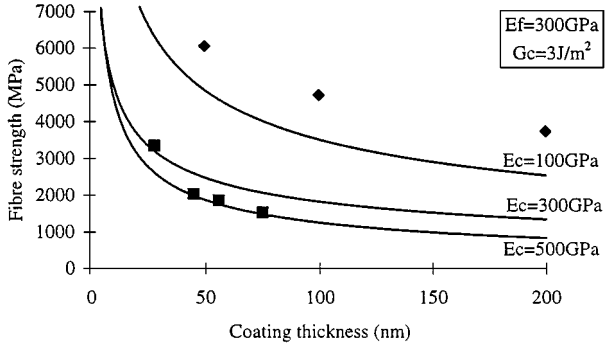

Figure 7 Experimental fibre strength evolution as a function of the coating thickness for TiB_2 (■ $E_{TiB2} = 500$ GPa) and C_{pyr} (♦ $E_{Cpyr} = 30$ GPa) single layers (present work) compared to calculated values from the extended Ochiai's model with different coating Young's moduli [22].

influence on the coated fibre strength of a layer having a different Young's modulus as compared to that of the fibre. According to their estimates, a higher Young's modulus of the layer implies a further decrease in the strength of the coated fibre and vice-versa which is consistent with the C_{pyr} experimental values (Fig. 7). In the specific case of TiB_2 coatings, the difference between the moduli ($E_{TiB2} = 500$ GPa) only leads to an approximately 10% decrease in the coated fibre strength for small thicknesses, thereby justifying the use of Ochiai's first model [8].

Moreover, microstructural aspects of the crack propagation in the C_{pyr} coating may introduce a non negligible deviation with respect to the perfect circumferential cleavage crack model in a brittle layer (Fig. 5a). For instance, a series of small axial debondings observed within the C_{pyr} coating thickness and which occur during the radial crack propagation (Fig. 3), could affect the crack geometry and stress state at the interface of the fibre through a crack blunting phenomenon. These debondings do not seem to be able to propagate too far in the axial direction as shown in Fig. 3 and the distance between each of them, approximately 10 nm, seems to be of the order of the size of the small graphite domains observed in the C_{pyr} microstructure (crystallites size along the c-axis of about 3 nm from both X-ray diffraction analysis [10] and TEM observations). However, due to the fact that the extended Ochiai's model including the effect of Young's modulus ratio already explains the observed behaviour (Fig. 7), these microstructural aspects of the crack propagation may be considered as ancillary effects.

3.2. $TiB_2 + C_{pyr}$ coated fibres

In the three investigated cases of double layer coated fibres (Table I), an increase in the mean strength as compared to the only TiB_2 coated fibres is observed, even for 150 nm thick TiB_2 coatings. The first two cases, with 50 nm and 125 nm C_{pyr} thick layers, and for which the TiB_2 thicknesses are similar, clearly indicate that the presence of even a very thin layer of C_{pyr} is sufficient to markedly improve the double coated fibre strength. Although this is further increased with a thicker C_{pyr} coating, the higher mean tensile strength does not attain the values measured on uncoated fibres, i.e. about 5400 MPa.

In the last two cases, with 125 nm C_{pyr} thick layers, and TiB_2 coatings which are about 75 nm and 150 nm thick, both tensile strength distributions seem to reveal the presence of essentially two populations of defects (Fig. 8). In both cases, the higher strength populations approximately coincide with the level observed for the uncoated fibres. Nevertheless, the presence of a second population of defects, located towards weaker strengths and which seems to be influenced by the TiB_2 thickness, may explain the decrease in the mean tensile strength determined using a unimodal description of the whole distribution (Table I). In fact, for the 125 nm C_{pyr} thickness, the most damaging population of defects with a 75 nm thick TiB_2 layer is centred about 4300 MPa whereas for a 150 nm thick TiB_2 layer, this population is located about 2800 MPa. It is worth noting that this last population of defects does not coincide with that observed with monofilaments only coated with

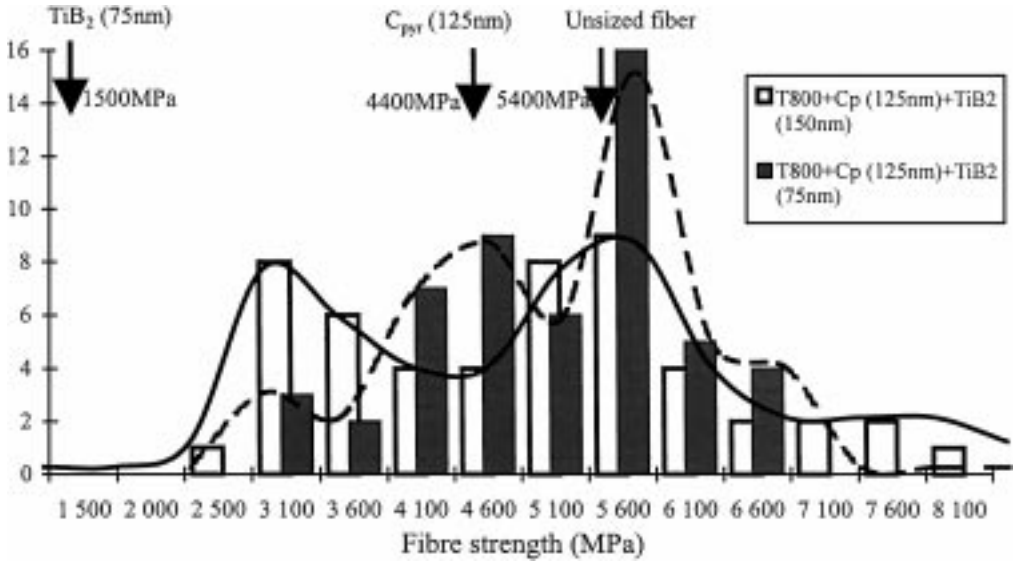

Figure 8 Tensile strength distribution for T800 fibres coated by C_{pyr} (125 nm) + TiB_2 (150 nm) or C_{pyr} (125 nm) + TiB_2 (75 nm).

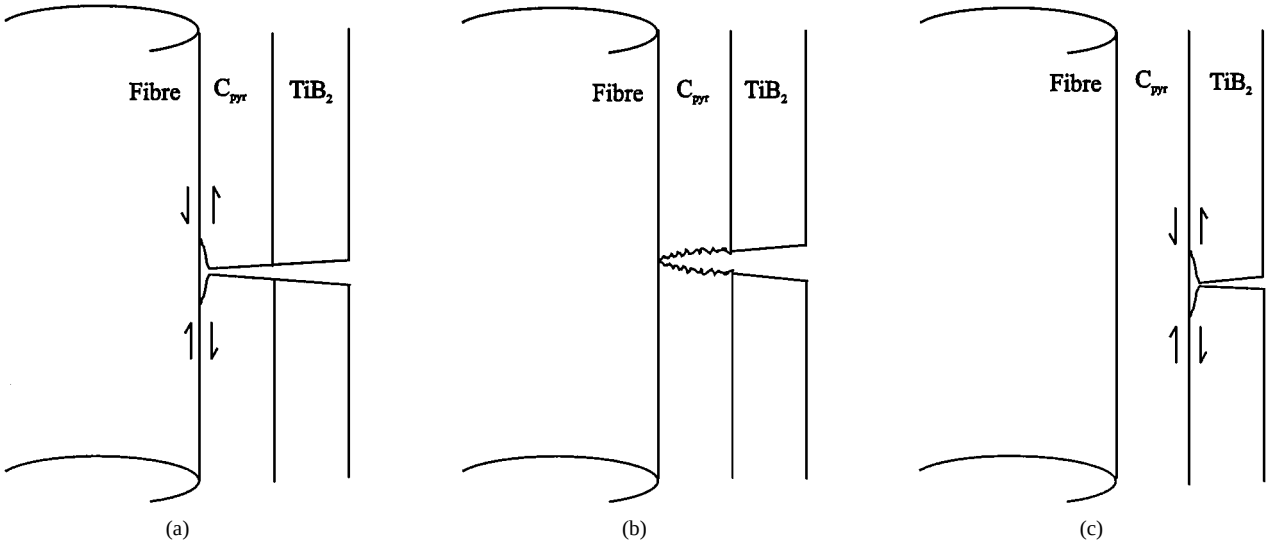

Figure 9 Schematic description of the crack propagation modes in the double coatings: (a) debonding at the fibre-C_{pyr} interface, (b) crack blunting, (c) debonding at the C_{pyr}-TiB_2 interface.

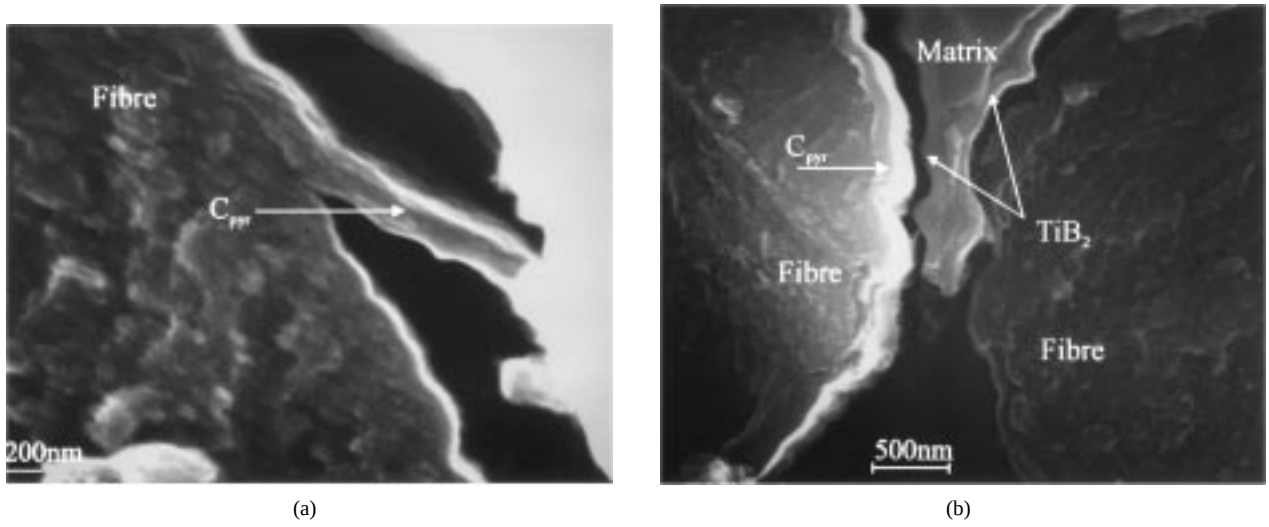

Figure 10 Failure surfaces of Al 10% wt Mg composite showing debondings at the C_{pyr}/fibre interface (a) and at the TiB_2/C_{pyr} interface (b).

TiB_2 (about 1500 MPa) thus excluding a defective C_{pyr} infiltration.

The above-mentioned populations may be related to the specific propagation modes of a circumferential crack in a double layer coating under the combined effect of internal thermal stresses and of the applied stress. For instance, the initiation of debonding cracks at the interfaces between the various phases is facilitated by the shear stress component resulting from the introduction of a free surface (crack propagation) in an internal stress field (Fig. 9a and c). These debonding phenomena, difficult to observe on the tested coated monofilaments, have been evidenced in an Al-10 wt% Mg composite at the interfaces between either the C_{pyr} coating and the fibre, or the TiB_2 and the C_{pyr} coatings (Fig. 10a and b). Although the internal thermal stresses cannot easily be compared to those in the coated monofilaments, the weak interface bondings thus evidenced may lead to the same debondings in the monofilaments. Moreover, the possible crack blunting inside the C_{pyr} layer, due to the typical C_{pyr} microstructure as already suggested in Section 3.1, could be further promoted by the tensile and shear thermal stresses resulting from the presence of the TiB_2 layer (Fig. 9b). The double layer may thus be assimilated to a thicker medium, in a reduced thermal stress field, having the properties of C_{pyr} so far as the crack propagation is concerned.

Consequently, the fact that some of the tested fibres coated with the double layer keep the uncoated fibre properties could be explained by a possible debonding at the interface between the C_{pyr} coating and the fibre thus eliminating the notch effect due to the cracked layer (Fig. 9a). This debonding mechanism is not observed in the case of a single C_{pyr} layer and this supports the explanation relative to the influence of the thermal stresses resulting from the presence of the TiB_2 layer in crack propagation modes.

Concerning the lower strength population of defects observed with 125 nm thick $C_{pyr} + 75$ nm thick TiB_2 coatings, the fact that the mean strength (about 4300 MPa) coincides with that of only C_{pyr} coated fibres suggests that the failure of the double coated fibre

is governed by the effect of the C_{pyr} coating itself. It may correspond to debonding between the TiB_2 and the C_{pyr} layers (Fig. 9c).

As regards the lowest mean strength population (about 2800 MPa), observed with 150 nm thick TiB_2 layer, it, in fact, coincides with the Ochiai's notch effect model corresponding to a C_{pyr} single layer having the thickness of both coatings (Fig. 9b). The absence of a strength population centred about 4300 MPa corresponding to debonding between the TiB_2 layer and the C_{pyr} coating is in good agreement with the previous hypothesis of a thick continuous layer.

4. Conclusion

This investigation was undertaken in order to evaluate the possible damage caused by protective coatings, such as pyrolytic carbon (C_{pyr}), TiB_2 and $C_{pyr} + TiB_2$ double layer, deposited on T800H carbon fibres. Tensile tests were carried out on uncoated and coated monofilaments in order to follow the fibre strength evolution.

In the case of the single TiB_2 film, the ceramic coating produces a noticeable strength decrease as a function of the layer thickness. Even for very small thicknesses such as 30 nm, a 35% drop with respect to the initial fibre properties, is measured. The fact that experimental data are in good agreement with the Ochiai's model, seems to indicate that the failure mechanism is controlled by the propagation of cracks in the fibre, initiated in the coatings. According to this analytical model, we deduced the maximum thickness, about 10 nm, under which no degradation should occur. This result implies that a single TiB_2 layer can hardly be envisaged as an interphase in composite applications given the processing difficulty involved in obtaining uniform thicknesses in this range.

Concerning the C_{pyr} coating, we observed that a thin film, about 50 nm in thickness, allows a 20% increase in fibre strength as compared to uncoated fibres. This phenomenon most probably results from the surface defects elimination induced by the coating. However, greater thicknesses lead also to a decrease in the monofilament tensile strength, as compared to the uncoated fibre, but less important than that observed for only TiB_2 coated fibres. These discrepancies are attributed to the differences between the elastic properties of the layers.

In the case of the double $C_{pyr} + TiB_2$ layer, the presence of C_{pyr} seems to preserve the properties of the uncoated fibre by allowing debonding at the interface between the fibre and the C_{pyr} coating. Although we notice a slight decrease in strength, it appears possible to optimize the C_{pyr} thickness in order to promote the crack deviation function of this layer while maintaining the required TiB_2 chemical barrier efficiency.

Acknowledgements

The authors would like to express their gratitude to Dr C. Diot (X-ray diffraction), M. Raffestin and D. Boivin (SEM images).

References

1. H.-S. YOON and A. OKURA, *SAMPE J.* **26**(3) (1990) 19.
2. M. RABINOVITCH, M.-H. VIDAL-SETIF, J.-C. DAUX, J.-L. RAVIART, J.-L. GERARD, R. MEVREL, M. LANCIN and O. PEREZ in Proceedings ICCM9, Madrid, Spain, edited by A. Miravete (Univ. Zaragoza, Spain, Woodhead Publ. Ltd. Cambridge, England, 1993) Vol. 1, p. 683.
3. G. D. ZHANG, S. R. FENG, Q. LI, J. T. BLUCHER and J. A. CORNIE, in "Controlled Interphases in Composite Materials," edited by H. Ishida (Elsevier, New York, 1990) p. 343.
4. A. SHINDO and K. HONJO, in Proceedings of the Third Japan-U.S. Conference on Composite Materials, Composites'86: Recent advances in Japan and the United States, edited by K. Kawata, S. Umekawa and A. Kobayashi (The Japan Society for Composite Materials, Tokyo, Japan, 1986) p. 767.
5. M. F. AMATEAU, *J. Comp. Mater*. **10** (1976) 279.
6. T. M. BESMANN, J. H. MILLER, K. M. COOLEY, R. A. LOWDEN and T. L. STARR, *J. Amer. Ceram. Soc*. **77** (1994) 2395.
7. A. G. METCALFE, *J. Comp. Mater.* **1** (1967) 356.
8. S. OCHIAI and Y. MURAKAMI, *J. Mater. Sci*. **14** (1979) 831.
9. M.-H. VIDAL-SETIF and J.-L. GERARD, in Proceedings Euro CVD 8, Glasgow, Scotland, edited by M. L. Hitchman and N. J. Archer (Les Editions de Physique, Les Ulis, France, 1991), *J. Phys. IV* **1**, C2-681.
10. P. BERTRAND, M.-H. VIDAL-SETIF and R. MEVREL, *Surf. Coating Techn*. **96** (1997) 283.
11. P. BERTRAND, M.-H. VIDAL-SETIF and R. MEVREL, in Proceedings Euro CVD 10, Venice, Italy, edited by G. A. Battiston, R. Gerbasi and M. Porchia (Les Editions de Physique, Les Ulis, France, 1995), *J. Phys. IV* **5**, C5-769.
12. O. PEREZ, G. PATRIARCHE, M. LANCIN and M.-H. VIDAL-SETIF, in Proceedings EUROMAT 93, Paris, France, edited by R. Pichoir and C. Costa (Les Editions de Physique, Les Ulis, France, 1993), *J. Phys. IV* **3**, C7-1693.
13. P. BERTRAND, Doctorate thesis, Paris XI (Orsay) University, 1996.
14. J.-C. DAUX, Dipl. Ing. Dissertation, CNAM, Paris, 1991.
15. W. WEIBULL, *J. Appl. Mech*. **18** (1951) 293.
16. B. BERGMAN, *J. Mater. Sci. Lett*. **3** (1984) 689.
17. S. VAN DER ZWAAG, *J. Test. Evaluat.* **17** (1989) 292.
18. K. TRUSTRUM and A. DE S. JAYATILAKA, *J. Mater. Sci.* **14** (1979) 1080.
19. K. HONJO and A. SHINDO, in "Composite Interfaces," edited by H. Ishida and J. L. Koenig (Elsevier, New York, 1986) p. 101.
20. T. HELMER, H. PETERLIK and K. KROMP, *J. Amer. Ceram. Soc*. **78** (1995) 133.
21. H. TADA, P. C. PARIS and G. R. IRWIN, "The Stress Analysis of Cracks Handbook" (Del Research Corporation, Hellertown, Pennsylvania, 1973).
22. S. OCHIAI, K. OSAMURA and K. HONDO, *Mater. Sci. Eng*. **A154** (1992) 149.
23. G. H. MILLER, *IEEE Trans. Magnetics* **17** (1981) 1032.
24. J. RAPPENEAU, M. YVARS, M. BOCQUET, C. DAVID and A. AURIOL, *Carbon* **2** (1964) 149.

Received 26 March 1997
and accepted 18 September 1998